Nucleon-nucleon and nucleon-Δ-isobar forces in a Skyrme model with higher derivative terms

T. Otofuji, S. Saito, and M. Yasuno
Department of Physics, Nagoya University, Nagoya 464, Japan

T. Kurihara and H. Kanada
Department of Physics, Niigata University, Niigata 950-21, Japan
(Received 30 June 1986)

The static properties of the skyrmion and the skyrmion-skyrmion (SS) interaction are investigated within a modified Skyrme model in which the symmetric quartic and the ω-coupling terms are both included. We approximate the latter term by the infinitely large limit for the ω-meson mass. The model is considered to be an effective Lagrangian of pions at low energies. A good agreement of the static properties of the nucleon is obtained using the coupling constants to fit the $\pi\pi$ scattering data. The SS interaction potential is expressed by means of the generalized spin and isospin operators. As a result, the potential is easily projected onto the potentials for NN, NΔ, and ΔΔ states with definite spin and isospin. It is shown that the SS potential has a good correspondence with the one-boson-exchange potential of the π and ρ mesons at large distances. The symmetric quartic term, which is necessary to achieve agreement with the S- and D-wave $\pi\pi$ scattering data, has been expected to give rise to an "σ-meson"-like attractive contribution at the intermediate range of the central potential. There exists, however, no such contribution, even if the strength of the symmetric quartic term is increased. This is because we must also increase the ω-coupling term to stabilize the skyrmion. We need further study of this problem.

I. INTRODUCTION

The Skyrme model[1] is now considered to be a candidate for low-energy effective theories of mesons and baryons, which may be derived from the large N_c limit of QCD. The model is essentially a nonlinear sigma model and involves a fourth-order derivative term $\mathcal{L}_{4A}$ called the Skyrme term. One needs the term to stabilize the soliton solution identified as the nucleon (N) or the delta isobar (Δ). The static properties of the nucleon can be explained[2] by the model up to an error of 30%.

The NN interaction has also been investigated[3–7] by means of the Skyrme model, and the skyrmion-skyrmion (SS) interaction potential has been shown to possess characteristics of the NN interaction: The long-range part of the SS potential is quite similar to that of the one-π and -ρ exchange model with reasonable values of the coupling constants $g_{\pi NN}$ and $g_{\rho NN}$, and its inside part has a repulsive core of the order of the nucleon mass. There exists, however, no attractive contribution at the intermediate range of the central potential. This means that the model shows no "σ-meson" exchange in their interaction.

With a view to remedy the above defect, Jackson *et al.*[8] proposed a modified Skyrme model in which the sign of the Skyrme term was inverted and a new stabilizer, which is a sixth-order term, $\mathcal{L}_6$, of the field derivative, was introduced. The term is just the ω-meson coupling term of Adkins *et al.*,[9] but with the infinitely large limit of the ω-meson mass. Although the modified model predicts such an attractive contribution, the negative sign of the Skyrme term does not agree with the $\pi\pi$ scattering data.

It is known that there exist two independent quartic terms in the chiral symmetry limit of meson Langrangian.[10] One is the antisymmetric term, just the Skyrme term, and the other is the symmetric term denoted by $\mathcal{L}_{4S}$. Donoghue *et al.*[11] showed that both quartic terms are necessary to reproduce the $\pi\pi$ scattering data at low energies, by examining the D-wave scattering lengths of $I=0$ and 2. Following the analysis, the Paris group[12] showed that the symmetric quartic term yields a contribution of the "σ-meson" exchange into the SS central potential. The term is, however, known to destabilize the soliton solution, so that we need a new stabilizing term in addition to the Skyrme term. For this purpose, we may use the ω-coupling term or the $\mathcal{L}_6$ term.

In the present paper we examine the SS interaction within the modified Skyrme model in which both the quartic terms, $\mathcal{L}_{4A}$ and $\mathcal{L}_{4S}$, and the sixth-order term, $\mathcal{L}_6$, are all included. The coupling constants in the model are chosen so as to reproduce the experimental $\pi\pi$ scattering data for the D waves and to achieve overall agreement between the static properties of the nucleon. In addition to this, we also consider the case without the $\mathcal{L}_{4S}$, for clarifying the role. The Paris group[13] and Eisenberg *et al.*[14] recently investigated the SS interaction by including the ω-coupling term. In the analyses they employed an additive ansatz for the ω field. We found that the ansatz is not good in predicting the short-range part of the potential. Instead of including the ω-coupling term, we decided to use the $\mathcal{L}_6$ term and calculate all the contributions from the term. The calculated SS potential

is projected onto the NN, NΔ, and ΔΔ channels by using an SO(4) tensor decomposition technique. We also develop a method of decomposing the interaction potential into terms with different asymptotic forms and G parities. This decomposition is very convenient for the discussion of what ingredients are involved in the potential.

The organization of this paper is as follows. In Sec. II the effective Lagrangian of our model is introduced. In Sec. III we describe a general form of the SS potential. The interaction potential is then projected onto those for the physical states of the nucleon and the delta isobar by means of generalized spin and isospin operators. Also, the asymptotic property of the potential is discussed. In Sec. IV we determine the coupling constants of the effective Lagrangian in conjunction with the $\pi\pi$ scattering data and calculate the static properties of the nucleon. The calculated radial dependence of the SS potential is given in this section, and its detailed structure and the G-parity dependence are discussed. We compare the resulting potential with a one-boson (π and ρ mesons) exchange potential and extract the coupling constants and the masses of the "exchanged π and ρ mesons." In Sec. V the summary of this paper and discussions are given.

II. MODIFIED SKYRME MODEL

We start with the following Lagrangian, considered an effective Lagrangian of QCD at low energies:

$$\mathcal{L}=\mathcal{L}_2+\mathcal{L}_{4A}+\mathcal{L}_{\chi SB}+\mathcal{L}_{4S}+\mathcal{L}_6 , \tag{2.1}$$

where $\mathcal{L}_2$, $\mathcal{L}_{4A}$, and $\mathcal{L}_{\chi SB}$ are the kinetic, Skyrme, and chiral symmetry breaking terms, respectively:

$$\begin{aligned}\mathcal{L}_2&=-\frac{F_\pi^2}{16}\mathrm{Tr}(L_\mu L^\mu) ,\\ \mathcal{L}_{4A}&=\frac{1}{32e^2}\mathrm{Tr}\{[L_\mu,L_\nu]^2\} ,\\ \mathcal{L}_{\chi SB}&=\frac{m_\pi^2 F_\pi^2}{8}\mathrm{Tr}(U-1) .\end{aligned} \tag{2.2}$$

Here, U is the SU(2) chiral field, and we used the notations for the left- and right-hand currents as $L_\mu=U^\dagger\partial_\mu U=i\tau_a L_\mu^a$ and $R_\mu=U\partial_\mu U^\dagger=i\tau_a R_\mu^a$. F_π denotes the pion decay constant, m_π the mass of pion, and e the coupling constant of the Skyrme term.

In Eq. (2.1), $\mathcal{L}_{4S}$ is the symmetric quartic term:

$$\mathcal{L}_{4S}=\left[\frac{\gamma}{8e^2}\right][\mathrm{Tr}(\partial_\mu U\partial^\mu U^\dagger)]^2 . \tag{2.3}$$

As shown by Gasser *et al.*[10] and Donoghue *et al.*,[11] the $\mathcal{L}_{4S}$ term is necessary to reproduce the low-energy $\pi\pi$ scattering data: The scattering lengths a_l^I of the $\pi\pi$ scattering are given by

$$\begin{aligned}a_0^0&=\frac{7m_\pi^2}{32\pi F_\pi^2} ,\\ a_2^0&=\frac{1}{30\pi e^2 F_\pi^2}(\gamma+\tfrac{1}{2}) ,\end{aligned} \tag{2.4}$$

and

$$a_2^2=-\frac{1}{30\pi e^2 F_\pi^2}(\gamma-\tfrac{1}{4}) .$$

To reproduce the experimental values of the scattering lengths, we obtain $0.1\lesssim\gamma\lesssim 0.2$. Recently, Pham *et al.*[15,16] used a dispersion theoretic approach to determine the $\pi\pi$ scattering and obtained $\gamma\sim 0.28$–0.34 to fit the S-wave $\pi\pi$ scattering. We see that the coupling constant γ is uncertain but not necessarily zero. The Paris group interpreted the $\mathcal{L}_{4S}$ term as a limit of a scalar meson coupling term for the infinitely large mass of the meson.[13]

The $\mathcal{L}_6$ term in Eq. (2.1) is the infinitely large mass limit of an ω-coupling term:

$$\mathcal{L}_6=-\frac{\epsilon_6^2}{4}B_\mu B^\mu , \tag{2.5}$$

where B_μ is the topological baryon current

$$B^\mu=\frac{1}{24\pi^2}\epsilon^{\mu\nu\alpha\beta}\mathrm{Tr}[L_\nu L_\alpha L_\beta] . \tag{2.6}$$

The parameter ϵ_6 in Eq. (2.5) is related to the ω-meson coupling constant g_ω by[9]

$$\epsilon_6^2=8\pi(g_\omega^2/4\pi)/m_\omega^2 . \tag{2.7}$$

The term $\mathcal{L}_6$ plays a role in stabilizing the soliton solution when we include $\mathcal{L}_{4S}$ with large coupling constant γ. There exists a critical coupling constant γ_c of the term $\mathcal{L}_{4S}$ such that we have no stable solution when $\gamma>\gamma_c$. We can find an upper limit of γ_c as follows:[15–17]

$$\gamma_c<\frac{1}{3}+\left[\frac{\delta}{27}\right]^{1/2} , \tag{2.8}$$

where $\delta=e^4F_\pi^2\epsilon_6^2/16\pi^4$. Numerically, γ_c is smaller than the value expected from the right hand side of Eq. (2.8).

Following the Skyrme ansatz, we write the static soliton solution as $U_0=\exp[iF(x)\tau\cdot\hat{\mathbf{x}}]$ for the chiral field U in Eq. (2.1). The solution with the unit baryon number is obtained by imposing the boundary condition on the chiral angle: $F(0)=\pi$ and $F(\infty)=0$. To describe the classical soliton as a quantum particle, we use the collective coordinate method introduced by Adkins *et al.*;[2] the physical solution is given by $U\equiv AU_0A^\dagger$, where A is a time-dependent but spatial-independent SU(2) matrix ($A=a_0+i\mathbf{a}\cdot\tau$ with $\sum_{i=0}^3 a_i^2=1$). The canonical quantization gives that the skyrmion can be quantized as the states with $J=I=\frac{1}{2},\frac{3}{2},\ldots$. The spin J and isospin I operators are described using the collective coordinates a_i:

$$\begin{aligned}J_k&=\frac{i}{2}\left[a_k\left[\frac{\partial}{\partial a_0}\right]-a_0\left[\frac{\partial}{\partial a_k}\right]-\epsilon_{klm}a_l\left[\frac{\partial}{\partial a_m}\right]\right] ,\\ I_k&=\frac{i}{2}\left[a_0\left[\frac{\partial}{\partial a_k}\right]-a_k\left[\frac{\partial}{\partial a_0}\right]-\epsilon_{klm}a_l\left[\frac{\partial}{\partial a_m}\right]\right] .\end{aligned} \tag{2.9}$$

The spin and isospin structure of the skyrmion is represented by the SO(3) matrix $D_{ij}(A)$, where $D_{ij}(A)=\mathrm{Tr}\{\tau_i A\tau_j A^\dagger\}/2$. The commutation relations of D_{ij} with the spin and isospin operators are given as follows:

$$[J_i,D_{kl}]=i\epsilon_{ilm}D_{km},\quad [I_i,D_{kl}]=i\epsilon_{ikm}D_{ml}\ . \tag{2.10}$$

Thus, the first index of D_{ij} denotes the isospin index, while the second denotes the spin index. Since these D_{ij}'s commute with each other, D_{ij}'s satisfy the same Lie algebra of the group as that for a symmetric pseudoscalar-meson theory in the strong coupling limit.[18–21] We describe this point in detail in Appendix A.

Integrating the Lagrangian in Eq. (2.1), we obtain

$$L=\int \mathscr{L}\,d\mathbf{x}=-M+\lambda\,\mathrm{Tr}[\dot{A}\dot{A}^{\dagger}]\ , \tag{2.11}$$

where the terms higher than the second orders of the time derivatives are neglected because the skyrmion is assumed to rotate slowly. In Eq. (2.11), M is the classical soliton mass:

$$M=\frac{F_\pi}{e}\frac{\pi}{2}\int_0^\infty d\tilde{r}\left[\tilde{r}^2\left[F'^2+\frac{2s^2}{\tilde{r}^2}\right]+4s^2\left[\frac{s^2}{\tilde{r}^2}+2F'^2\right]-4\gamma\tilde{r}^2\left[F'^2+\frac{2s^2}{\tilde{r}^2}\right]^2+2\delta\frac{s^4}{\tilde{r}^2}F'^2+2\beta^2\tilde{r}^2(1-c)\right]\ , \tag{2.12}$$

where $\tilde{r}=eF_\pi r$, $\beta=m_\pi/(eF_\pi)$, $s=\sin F$, and $c=\cos F$. In Eq. (2.11), λ is the moment of inertia of the rotating skyrmion:

$$\lambda=\frac{F_\pi}{e}\frac{2\pi}{3}\int_0^\infty \tilde{r}^2 d\tilde{r}\,s^2\left[1+4\left[F'^2+\frac{s^2}{\tilde{r}^2}\right]-8\gamma\tilde{r}^2\left[F'^2+\frac{2s^2}{\tilde{r}^2}\right]+4\delta\frac{s^4}{\tilde{r}^2}F'^2\right]\ . \tag{2.13}$$

The chiral angle $F(r)$ is the solution of the following Euler-Lagrange equation:

$$\left[\frac{\tilde{r}}{4}+2(1-2\gamma)s^2-6\gamma\tilde{r}^2F'^2+\delta\frac{s^4}{\tilde{r}^2}\right]F''+\left[\frac{\tilde{r}}{2}-2\delta\frac{s^2}{\tilde{r}^3}\right]F'-\frac{sc}{2}$$
$$+\left[2(1-2\gamma)sc+2\delta\frac{s^3c}{\tilde{r}^2}\right]F'^2-4\gamma\tilde{r}F'^3-(1-4\gamma)\frac{2s^3c}{\tilde{r}^2}-\frac{\beta^2}{4}\tilde{r}^2s=0\ . \tag{2.14}$$

III. SKYRMION-SKYRMION INTERACTION

A. Definition of the SS potential

For a two-skyrmion system, we assume a product form for its chiral field as follows:

$$U(\mathbf{x};\mathbf{X}_1,\mathbf{X}_2)=A_1U_0(\mathbf{x}-\mathbf{X}_1)A_1^{\dagger}A_2U_0(\mathbf{x}-\mathbf{X}_2)A_2^{\dagger}\ , \tag{3.1}$$

where $\mathbf{X}_1$ and $\mathbf{X}_2$ are the coordinate parameters denoting the centers of two skyrmions, and A_1 and A_2 are the collective coordinates to describe their spinning motions. Substituting Eq. (3.1) into Eq. (2.1), we obtain the following Hamiltonian:

$$\mathscr{H}(\mathbf{x};\mathbf{X}_1,\mathbf{X}_2,A_1,A_2)=\mathscr{H}_1(\mathbf{x};\mathbf{X}_1,A_1)+\mathscr{H}_1(\mathbf{x};\mathbf{X}_2,A_2)$$
$$+\mathscr{H}_{\rm int}(\mathbf{x};\mathbf{X}_1,\mathbf{X}_2,A_1,A_2)\ , \tag{3.2}$$

where $\mathscr{H}_1$ is the Hamiltonian of the two skyrmions, and $\mathscr{H}_{\rm int}$ denotes the rest interpreted as their interaction part. From now on we neglect the time-derivative terms in $\mathscr{H}_{\rm int}$, since the rotation of the skyrmions is considered to be slow.

The SS potential is obtained by integrating $\mathscr{H}_{\rm int}$ in Eq. (3.2). The resulting potential is written as the sum of the contributions from the respective terms in the effective Lagrangian in Eq. (2.1) as follows:

$$V=\int d\mathbf{x}\,\mathscr{H}_{\rm int}(\mathbf{x};\mathbf{X}_1,\mathbf{X}_2,A_1,A_2)$$
$$=V_{\chi\rm SB}+V_2+V_{4A}+V_{4S}+V_6\ , \tag{3.3}$$

where $V_{\chi\rm SB}$, V_2, V_{4A}, V_{4S}, and V_6 denote those from the terms $\mathscr{L}_{\chi\rm SB}$, $\mathscr{L}_2$, $\mathscr{L}_{4A}$, $\mathscr{L}_{4S}$, and $\mathscr{L}_6$ in Eq. (2.1), respectively. Each V_i ($i=\chi$SB, 2, 4A, 4S, and 6) has the three components which are asymptotically those of the one-, two-, and three-pion exchange potentials, and are referred as $V_i^{\rm I}$, $V_i^{\rm II}$, and $V_i^{\rm III}$, respectively. The potentials are explicitly written as follows: The χSB term yields

$$V_{\chi\rm SB}^{\rm I}(\mathbf{r})=\frac{m_\pi^2F_\pi^2}{108}\int d\mathbf{x}\,u_i(1)\hat{D}_{ij}u_j(2)\ , \tag{3.4a}$$

$$V_{\chi\rm SB}^{\rm II}(\mathbf{r})=-\frac{m_\pi^2F_\pi^2}{4}\int d\mathbf{x}[u_0(1)-1][u_0(2)-1]\ ,$$

where u_0 and u_i are defined by

$$U_0(\mathbf{x}-\mathbf{X}_j)=u_0(j)+i\tau_iu_i(j),\quad j=1\text{ or }2 \tag{3.4b}$$

and $\hat{D}_{ij}$ is the SO(3) representation matrix of the argument $A_1^{\dagger}A_2$ as follows:[4]

$$\hat{D}_{ij}\equiv D_{ij}(A_1^{\dagger}A_2)\ . \tag{3.5}$$

Throughout this paper, the repeated indices mean the summation over 1 , 2 and 3. The kinetic term has only the $V_2^{\rm I}$ component,

$$V_2^{\rm I}(\mathbf{r})=\frac{F_\pi^2}{216}\int d\mathbf{x}[(\tilde{R}L)+(R\tilde{L})]\ , \tag{3.6}$$

where the parentheses in the integrand means $(AB)=A_j^iB_j^i$, and the following notations R_k^i and L_k^i were used for brevity's sake:

$$R_k^i \equiv \mathrm{Tr}\{\tau_i U_0(1)\partial_k U_0^\dagger(1)\}/(2i) ,$$
$$L_k^i \equiv \mathrm{Tr}\{\tau_i U_0^\dagger(2)\partial_k U_0(2)\}/(2i) , \tag{3.7}$$

where $U_0(i)$ ($i=1$ and 2) stand for $U_0(\mathbf{x}-\mathbf{X}_i)$. All the expressions involve only the above combinations; that is, $\mathbf{X}_1$ appears through the right-hand current and $\mathbf{X}_2$ through the left-hand current. In Eq. (3.6), we have also used the following:

$$\tilde{R}^i_j \equiv R^k_j \hat{D}_{ki} \quad \text{and} \quad \tilde{L}^i_j \equiv \hat{D}_{ik} L^k_j . \tag{3.8}$$

The Skyrme term $\mathscr{L}_{4A}$ yields

$$V^{\mathrm{I}}_{4A}(\mathbf{r}) = \frac{1}{e^2}\int d\mathbf{x}[(RR\tilde{R}L)+(LL\tilde{L}R)] , \tag{3.9a}$$

$$V^{\mathrm{II}}_{4A}(\mathbf{r}) = \frac{1}{2e^2}\int d\mathbf{x}[(RRLL)+(\tilde{R}L\tilde{R}L)+(\tilde{R}LL\tilde{R})] , \tag{3.9b}$$

where we have defined

$$(ABCD) \equiv A^i_j B^i_j C^l_k D^l_k - A^i_j B^i_k C^l_j D^l_k . \tag{3.9c}$$

The symmetric quartic term $\mathscr{L}_{4S}$ gives

$$V^{\mathrm{I}}_{4S} = -\frac{\gamma}{e^2}\int d\mathbf{x}[(RR)(\tilde{R}L)+(LL)(\tilde{L}R)] , \tag{3.10a}$$

$$V^{\mathrm{II}}_{4S} = -\frac{\gamma}{e^2}\int d^3\mathbf{x}[2(RR)(LL)+(\tilde{R}L)(\tilde{R}L)] . \tag{3.10b}$$

The ω-coupling term $\mathscr{L}_6$ gives

$$V^{\mathrm{I}}_6(\mathbf{r}) = 6\left(\frac{\epsilon_6}{24\pi^2}\right)^2 \times \int d\mathbf{x}[(\tilde{R}LL)(LLL)+(\tilde{L}RR)(RRR)] , \tag{3.11a}$$

$$V^{\mathrm{II}}_6(\mathbf{r}) = 3\left(\frac{\epsilon_6}{24\pi^2}\right)^2 \times \int d\mathbf{x}[(RRR)(\tilde{R}LL)+2(LLL)(\tilde{L}RR) +3(\tilde{L}RR)(\tilde{L}RR)+3(\tilde{R}LL)(\tilde{R}LL)] , \tag{3.11b}$$

$$V^{\mathrm{III}}_6(\mathbf{r}) = 2\left(\frac{\epsilon_6}{24\pi^2}\right)^2 \times \int d\mathbf{x}[(RRR)(LLL)+9(RR\tilde{L})(LL\tilde{R})] , \tag{3.11c}$$

where we have defined

$$(ABC) \equiv \epsilon_{ijk}\epsilon_{lmn} A^l_i B^m_j C^n_k . \tag{3.12}$$

B. Tensor decomposition

In order to project the SS potential onto that for the physical nucleon and/or delta isobar states, we decompose the terms $\hat{D}_{ij}$ and $\hat{D}_{ij}\hat{D}_{kl}$ in the above expressions appearing through $\tilde{R}$ or $\tilde{L}$ into those of the SO(3) irreducible tensors:

$$\hat{D}_{ij} = \tfrac{1}{27}(\Theta_{T,ij} + \Theta_{ss}\delta_{ij})$$

and

$$\hat{D}_{ij}\hat{D}_{kl} = H^{(1)}_{ij}\delta_{kl} + H^{(1)}_{kl}\delta_{ij} + H^{(2)}_{ik}\delta_{jl} + H^{(2)}_{lj}\delta_{ik} + H^{(3)}_{il}\delta_{jk} + H^{(3)}_{kj}\delta_{il} + \delta_{ij}\delta_{kl}G^{(1)} + \delta_{ki}\delta_{jl}G^{(2)} + \delta_{kj}\delta_{il}G^{(3)} , \tag{3.13}$$

where H and G are expressed in terms of the SO(4) spin-isospin irreducible tensors Θ and Θ' as follows:

$$\begin{aligned} H^{(1)}_{ij} &= \tfrac{1}{378}(6\Theta'_{T,ij} - \Theta_{T,ij}) , \\ H^{(2)}_{ij} &= -\tfrac{4}{189}(\Theta'_{T,ij} + \Theta_{T,ij}) , \\ H^{(3)}_{ij} &= \tfrac{1}{378}(6\Theta'_{T,ij} + 13\Theta_{T,ij}) , \\ G^{(1)} &= \tfrac{1}{270}(3\Theta'_{ss} + 5\Theta_{ss}) , \\ G^{(2)} &= -\tfrac{1}{135}(\Theta'_{ss} - 45) , \\ G^{(3)} &= \tfrac{1}{270}(3\Theta'_{ss} - 5\Theta_{ss}) . \end{aligned} \tag{3.14}$$

Here, Θ_{ss} (Θ'_{ss}) and $\Theta_{T,ij}$ ($\Theta'_{T,ij}$) denote the zeroth- (second-) rank irreducible tensors, respectively, and are given by

$$\begin{aligned} \Theta_{ss} &= 9\hat{D}_{kk} , \\ \Theta'_{ss} &= 9(\hat{D}_{kk}\hat{D}_{ll} - \hat{D}_{kk} - 1) , \\ \Theta_{T,ij} &= 9(3\hat{D}_{ij} - \delta_{ij}\hat{D}_{kk}) , \\ \Theta'_{T,ij} &= 9(3\hat{D}_{ij} - \delta_{ij}\hat{D}_{kk})(\hat{D}_{ll} + \tfrac{1}{2}) . \end{aligned} \tag{3.15}$$

The matrix elements of $\hat{D}_{ij}$ between physical states are calculated as follows:

$$\langle B_1 B_2 \,|\, D_{ij}(A_1^\dagger A_2) \,|\, B'_1 B'_2 \rangle = \Lambda(B_1,B'_1)\Lambda(B_2,B'_2)(S_i)_1(S_j)_2(\mathbf{T}_1\cdot\mathbf{T}_2) , \tag{3.16a}$$

where B_i denotes the N or Δ state, and $\mathbf{S}$ and $\mathbf{T}$ are the generalized spin and isospin operators, respectively. $\Lambda(B,B')$ is a kind of reduced matrix element in the SU(2)×SU(2) matrix, and can be obtained using the strong coupling relation[18–21] as shown in Appendix A:

$$\begin{aligned} &\Lambda(\mathrm{N},\mathrm{N}) = -\tfrac{1}{3}, \quad \Lambda(\mathrm{N},\Delta) = \Lambda(\Delta,\mathrm{N}) = 1/\sqrt{2} , \\ &\Lambda(\Delta,\Delta) = -\tfrac{1}{15}, \quad \Lambda(\Delta,\tfrac{5}{2}) = \sqrt{3}/2 . \end{aligned} \tag{3.16b}$$

Summarizing the above, one can write the static potential between skyrmions in terms of a general operator form as follows:

$$V(\mathbf{r};A_1,A_2) = V_c(r) + \Theta_{ss}V_{ss}(r) + \Theta_T V_T(r) + \Theta'_{ss}V'_{ss}(r) + \Theta'_T V'_T(r) , \tag{3.17a}$$

where

$$\Theta_T = \Theta_{T,ij}\hat{r}_i\hat{r}_j \quad \text{and} \quad \Theta'_T = \Theta'_{T,ij}\hat{r}_i\hat{r}_j , \tag{3.17b}$$

with $\mathbf{r} = \mathbf{X}_1 - \mathbf{X}_2$ the relative coordinate between the skyrmions. Referring to Eqs. (3.15) and (3.16a), one notices that Θ_{ss} and Θ_T are the $(\boldsymbol{\sigma}\cdot\boldsymbol{\sigma})(\boldsymbol{\tau}\cdot\boldsymbol{\tau})$ and $S_{12}(\boldsymbol{\tau}\cdot\boldsymbol{\tau})$ terms for the NN potential, respectively. Θ'_{ss} and Θ'_T denote the

tensors consisting of the second-rank spin and isospin operators for each skyrmion. These tensors are thus only effective for the NΔ or ΔΔ states and not for the NN states. The existence of the higher-rank tensor terms were noted by Yabu *et al.*[6] independently.

C. Asymptotic form of the SS potential

From the above tensor decomposition of the potential, we notice that the V^{I} potentials involve only the Θ_{ss} and Θ_T dependences because they are linear in $\hat{D}_{ij}$. On the other hand, the potentials V^{II} and V^{III} involve all kinds of dependences that appeared in Eq. (3.17a). Now, let us see the asymptotic behavior of the V^{I} potentials. The chiral angle $F(r)$ behaves, in the asymptotic region, as

$$F(r)\to\chi\frac{\exp(-m_\pi r)}{m_\pi r} \quad \text{at } r\to\infty \ , \tag{3.18}$$

where the proportional factor χ is associated with the pseudoscalar coupling constant $g_{\pi\mathrm{NN}}$ as[6]

$$\chi=(3/4\pi)(m_\pi^2/M_{\mathrm{N}})(g_{\pi\mathrm{NN}}/F_\pi) \ . \tag{3.19}$$

Using this asymptotic form of $F(r)$, one obtains

$$V^{\mathrm{I}}\to\frac{9}{4\pi}\left[\frac{g_{\pi\mathrm{NN}}}{2M_{\mathrm{N}}}\right]^2 D_{ai}(A_1)D_{aj}(A_2)\partial_i\partial_j(e^{-m_\pi r}/r) \ . \tag{3.20}$$

From the matrix element given by Eq. (3.16a), we have the Sugawara–von Hippel form[22] for the potential:

$$\begin{aligned}\langle B_1B_2\,|\,V^{\mathrm{I}}\,|\,B_1'B_2'\rangle\to&\frac{m_\pi}{12\pi}\frac{m_\pi}{2M_{\mathrm{N}}}g_{\pi B_1B_1'}g_{\pi B_2B_2'}\\&\times\mathbf{T}_1\cdot\mathbf{T}_2[\mathbf{S}_1\cdot\mathbf{S}_2Y(m_\pi r)\\&+S_{12}Z(m_\pi r)] \ ,\end{aligned} \tag{3.21}$$

with

$$Y(x)=\frac{e^{-x}}{x}$$

and

$$Z(x)=\left[1+\frac{3}{x}+\frac{3}{x^2}\right]Y(x) \ . \tag{3.22}$$

Using Eqs. (3.16b), (3.19), (3.20), and (3.21), we obtain the following relations between the coupling constants:

$$g_{\pi\mathrm{N}\Delta}/g_{\pi\mathrm{NN}}=3/\sqrt{2} \ \text{ and } \ g_{\pi\Delta\Delta}/g_{\pi\mathrm{NN}}=1/5 \ . \tag{3.23}$$

The relations are just those derived from the strong coupling theory.

D. G-parity and $S\bar{S}$ potential

Now let us consider the skyrmion-antiskyrmion ($S\bar{S}$) potential. For this purpose, we make a G-parity transformation to one of the skyrmions; for example, we replace $U_0(\mathbf{x}-\mathbf{X}_1)$ in Eq. (3.1) with $U_0^\dagger(\mathbf{x}-\mathbf{X}_1)$. For such a transformation, $R_k^i(1)$ defined by Eq. (3.7) becomes $L_k^i(1)$, where the argument "1" means $U_0(\mathbf{x}-\mathbf{X}_1)$ to be the argument. After this replacement, we obtain the $S\bar{S}$ potential. However, we must symmetrize the result with respect to the particle coordinates, since the potential is linearly dependent on the relative coordinate; otherwise, the parity conservation is broken.

The G-parity structure of the SS potential can be seen easily from the above $S\bar{S}$ potential. In the expression of the $S\bar{S}$ potential, we can replace $L_k^i(1)$ in terms of $R_k^i(1)$ using the identity $L_k^i(1)=-R_i^k(1)$. We then note that the symmetric part of R_i^k in the suffixes i and k has an asymptotic form of the one-pion-exchange tail, and the antisymmetric part has that of the two-pion-exchange tail. Hence, if we consider a long-range behavior of the potential, the G-parity structure is determined by the powers of R_k^i in the expressions (3.6) and (3.9a)–(3.11c), because the symmetric part is only responsible for that behavior. Thus, V^{I} and V^{III} are odd in the G parity, and V^{II} is even in the G parity. This means that V^{I} and V^{III} has the character of the π or ω exchange, while V^{II} has that of the σ or ρ.

TABLE I. Calculated static properties of the nucleon.

Quantity	Case I	Case II	Case III	Experiment
F_π (MeV)	120	125	186	186
e	10.0	12.0	3.4	
γ_2	0.0	0.1	0.0	
$g_\omega^2/4\pi$	10.0	10.0	0.0	
M_{N} (MeV)	input	input	2131	938.9
M_Δ (MeV)	input	input	2294	1232.
$\langle r^2\rangle_{I=0}^{1/2}$ (fm)	0.76	0.74	0.58	0.72
$\langle r^2\rangle_{I=1}^{1/2}$ (fm)	1.07	1.04	0.93	0.88
$\langle r^2\rangle_{M,I=0}^{1/2}$ (fm)	0.98	0.94	0.82	0.81
μ_{p}	2.24	2.12	3.03	2.79
μ_{n}	−1.44	−1.33	−2.73	−1.91
$\lvert\mu_{\mathrm{p}}/\mu_{\mathrm{n}}\rvert$	1.55	1.59	1.11	1.46
$g_{\pi\mathrm{NN}}$	14.5	12.9	14.3	13.5
g_A	0.84	0.80	0.57	1.23

IV. NUMERICAL RESULTS

A. Static properties of the nucleon

Our model involves the parameters F_π, e, γ, and ϵ_6. F_π is the pion-decay constant, and e and γ are determined by the $\pi\pi$ D-wave scattering lengths in Eq. (2.4). ϵ_6 is related to the ω-meson coupling constant g_ω in Eq. (2.7). To achieve overall agreement with these data, we choose the parameters within the following:

$$\begin{aligned} &F_\pi = 120\text{–}186 \text{ MeV} , \\ &\gamma = 0.12\text{–}0.2 , \\ &e = 3.4\text{–}12 , \\ &\frac{g_\omega^2}{4\pi} = 5.0\text{–}10.0 . \end{aligned} \tag{4.1}$$

As stated in Sec. II, the experimental data are very uncertain, so these values of the parameters should not be taken seriously. To reproduce the $I=J=0$ scattering length of the $\pi\pi$ scattering in terms of the chiral symmetry breaking term $\mathcal{L}_{\chi SB}$, we must reduce the value of F_π considerably. This may not be so when we include the term $\mathcal{L}_{4S}$.

Within the above ranges of the parameters, we attempt to reproduce the masses of the nucleon and the delta isobar. We adopt the following two cases: Case I is for $F_\pi = 120$ MeV, $e=10.0$, $\gamma=0.0$, and $g_\omega^2/(4\pi)=10$; case II is for $F_\pi = 125$ MeV, $e=12.0$, $\gamma=0.1$, and $g_\omega^2/(4\pi)=10$. Case I was chosen for the case without the term $\mathcal{L}_{4S}$ ($\gamma=0$). In choosing case II ($\gamma\neq 0$), we tried to solve the differential equation in Eq. (2.14), but could not get any solution for the chiral angle $F(r)$ for $\gamma > 0.1$. As mentioned in Refs. 15 and 16, the term $\mathcal{L}_{4S}$ works as a strong destabilizer, so that γ must be smaller than a critical value. It can be shown that the inclusion of the term gives rise to an instability of multiskyrmion systems.[17] In this meaning we prefer case I, but as a phenomenological model we used the value $\gamma=0.1$ in case II. Later we discuss the case for large values of γ.

The static properties of the nucleon are calculated for the above two cases and are listed in Table I. For a reference, we also showed the case of the pure Skyrme model[7] with $\gamma=\epsilon_6=0$ (referred to case III), where F_π is taken to be the experimental value 186 MeV, and e is chosen so as

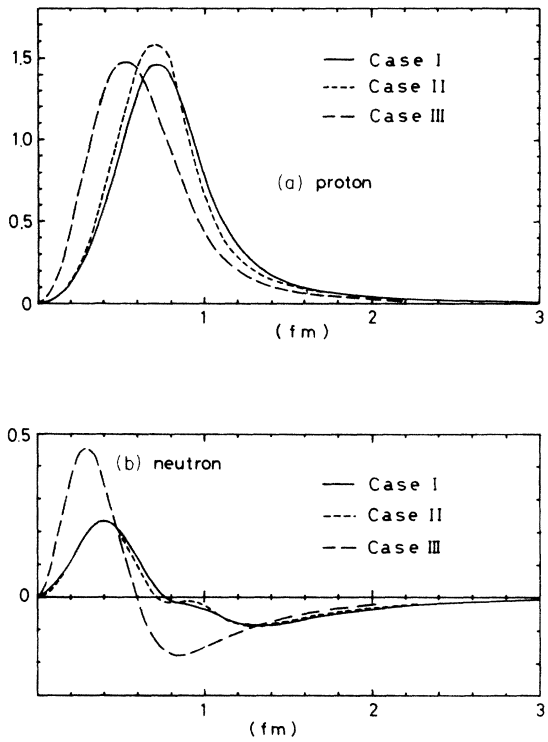

FIG. 2. The charge distributions of the proton and the neutron: (a) and (b) are for the proton and the neutron, respectively. See the caption of Fig. 1 for details.

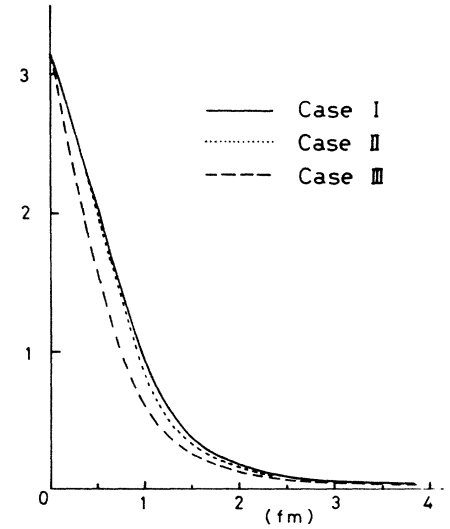

FIG. 1. The radial dependence of the calculated chiral angle $F(r)$: The solid, dotted, and dashed curves are the solutions for cases I, II, and III, respectively.

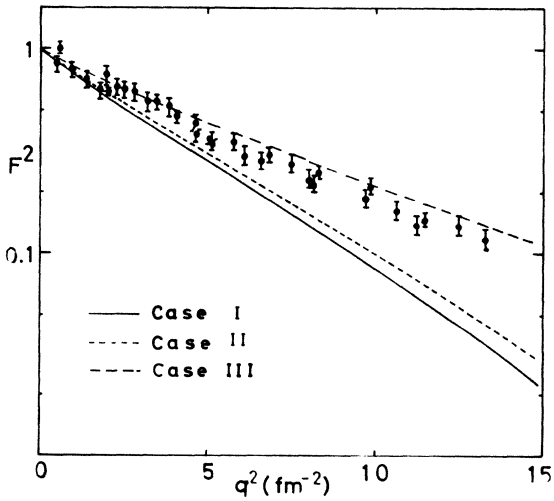

FIG. 3. The calculated charge form factor of the proton in a comparison with the experimental data (Ref. 23). See the caption of Fig. 1.

to reproduce the nucleon pion coupling constant $g_{\pi NN}$. From Table I one notices that the calculated static properties for cases I and II are in good agreement with experimental data. In Fig. 1 we show the radial dependence of $F(r)$. The figure shows that the chiral angles $F(r)$ for cases I and II swell in the intermediate range in comparison with that of case III. This effect is due to the ω-coupling term $\mathscr{L}_6$. Comparing case I with II we see that the effect of the $\mathscr{L}_{4S}$ term shrinks $F(r)$. The charge densities of the proton and neutron are shown in Fig. 2. The results for cases I and II are slightly shifted toward the outside region compared with case III. Figure 3 displays the calculated charge form factor of the proton in a comparison with the experimental data.[23] The agreement of the results for cases I and II is rather good at the low-momentum transfer region, although it is poor at high momentum. On the other hand, the result for case III is in good agreement with the data at the high momentum.

B. Skyrmion-skyrmion potential

Following the prescription described in Sec. III, we calculate the SS ($S\bar{S}$) potential. Figures 4(a), 4(b), and 4(c) show the calculated central V_c, spin-spin V_{ss}, and tensor V_T potentials for case I, respectively. In the figures the upper parts are for the SS potential, the lower for the $S\bar{S}$ potential. Similarly, the higher-rank spin-spin V'_{ss} and tensor V'_T potentials are shown in Figs. 4(d) and 4(e). The solid curves show the net contributions of the potentials. Each component is also displayed in the figures when its contribution is large: The long-dashed, short-dashed, and dotted curves display the contributions from $V_6^{\rm I}$, $V_6^{\rm II}$, and $V_6^{\rm III}$, respectively. Also, the dotted-dashed curve denote that from $V_2^{\rm I}$, and the double-dotted—dashed and triple-dotted—dashed curves denote those from the $V_{\chi SB}^{\rm I}$ and $V_{\chi SB}^{\rm II}$ terms, respectively. The contributions from the Skyrme term, V_{4A}, are rather small for case I, so the contributions are not shown in the figures.

For the central potential in Fig. 4(a), we see that $V_6^{\rm III}$ has odd G parity, and $V_6^{\rm II}$ and $V_{\chi SB}^{\rm II}$ have even G parity. This can be seen from the comparison with the potential for the $S\bar{S}$ interaction in the lower part of Fig. 4(a). Thus, $V_6^{\rm III}$ has a characteristic of the ω-meson exchange potential and is the main contribution to the short range part. The potential $V_6^{\rm III}$ has a simple structure; as seen from Eq. (3.10c), one can write for the central potential

$$V_6^{\rm III}(\mathbf{r})=\epsilon_6^2\int d\mathbf{x}\,B^0(\mathbf{x}-\mathbf{X}_1)B^0(\mathbf{x}-\mathbf{X}_2)\ , \tag{4.2}$$

where $B^0(\mathbf{x}-\mathbf{X}_i)$ $(i=1,2)$ denote that baryon densities around the centers $\mathbf{X}_i$. Equation (4.2) shows that the central part of $V_6^{\rm III}$ is just the folding of the baryon densities

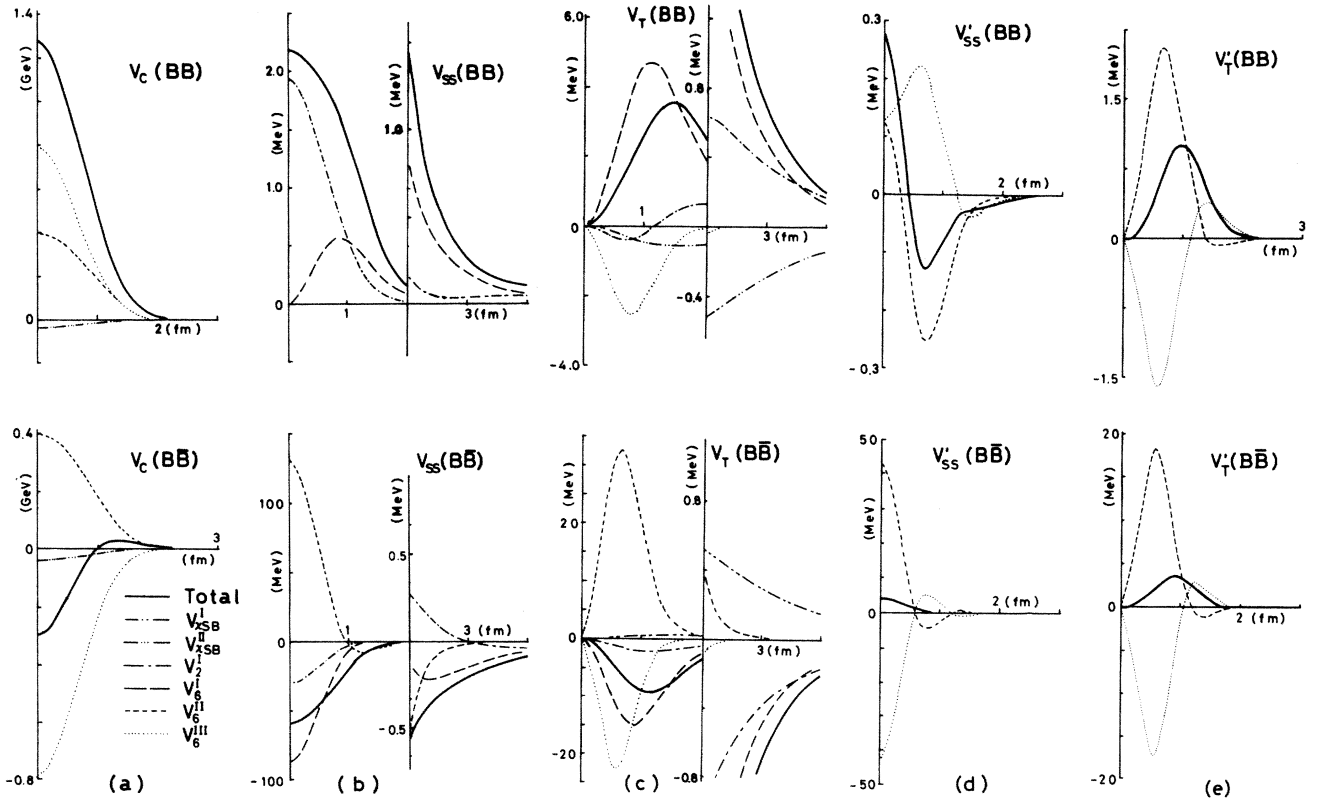

FIG. 4. The skyrmion-skyrmion (upper part) and skyrmion-antiskyrmion (lower part) potentials calculated for case I. (a), (b), and (c) are the central, V_c, the spin-spin, V_{ss}, and the tensor, V_T parts, respectively. (d) and (e) are the spin-spin, V'_{ss}, and the tensor, V'_T, parts of the higher rank, respectively. The solid curves are the net contributions. The dotted, dashed, and long-dashed curves denote the contributions from the terms $V_6^{\rm III}$, $V_6^{\rm II}$, and $V_6^{\rm I}$, respectively. The dotted-dashed, triple-dotted—dashed, and double-dotted—dashed curves show the contributions from the terms $V_2^{\rm I}$, $V_{\chi SB}^{\rm I}$, and $V_{\chi SB}^{\rm II}$, respectively.

of the skyrmions. This is because we used the infinitely large limit of the ω-meson mass for the ω-meson coupling term. On the other hand, $V^{II}_{\chi SB}$ and V^{II}_6 give the σ-meson-like exchange contributions. The former has a correct sign, but is small, and the latter has the incorrect sign.

For the spin-spin potential displayed in Fig. 4(b), we note that the contribution from V^I_2 dominates in the inside region, while that from V^I_6 dominates in the asymptotic region. (Note the breaks of the curves at $r=2$ fm. The scales of the vertical axes are the same at $r>2$ fm as for the upper and lower graphs.) Both contributions have odd G-parity structure in the outside region ($r>2.0$ fm). Compared with the previous result,[7] we note that the role of the Skyrme term V^I_{4A} in the pure Skyrme model has been replaced by that of the ω-coupling term V_6 in this case, and the net result is very similar to that of the pure Skyrme model.

For the tensor potential displayed in Fig. 4(c), V^I_6, $V^I_{\chi SB}$, and V^I_2 are the main contributions in the asymptotic region. In the same way as the spin-spin interaction, the G-parity structure of each component is clearly seen in comparison with that of the $S\bar{S}$ potential. Although each contribution is different, the net contribution is also similar to that of the pure Skyrme model.

For the potentials of the higher rank tensor, V'_{ss} and V'_T, shown in Figs. 4(d) and 4(e), we note that each component is rather large, while the net becomes small. We, however, discuss the contribution of V'_T to the potential between the NΔ states later.

C. Effect of the symmetric quartic term

Figures 5(a), 5(b), and 5(c) show the central, spin-spin, and tensor parts of the SS potential calculated for case II, respectively. In this case, the contribution V_{4S} from the symmetric quartic term, $\mathscr{L}_{4S}$, is included, and is depicted by the thin solid curve. Figure 5(a) shows that the $\mathscr{L}_{4S}$ contributes attractively, but is not sufficient to overcome the repulsive contribution from the ω-coupling term. The net result is purely repulsive, so that there is no sign of the σ-meson exchange in the intermediate region. For the spin-spin and the tensor part in Figs. 5(b) and 5(c), the contribution of the $\mathscr{L}_{4S}$ term is rather small.

D. Comparison with the OBE potential

To facilitate comparison with a one-boson-exchange (OBE) potential for the NN interaction, we calculate the ratios of the present results to those of the OBE potential:

$$R_j^-(r)=\frac{V_j^-(r)}{V_\pi^j(r)},\quad R_j^+(r)=\frac{V_j^+(r)}{V_\rho^j(r)}\quad (j=T \text{ or ss}), \tag{4.3}$$

where V^j_π and V^j_ρ denote the one-π and -ρ exchange potentials, respectively, and V_j^- (V_j^+) is the G-parity odd (even) component calculated from the SS and the $S\bar{S}$ potentials. If the calculated result is the same as that of the OBE, then the ratio $R^\pm_T/R^+_{ss}$ is independent of the coupling constant of the OBE potential. The calculated ratios for case I are shown in Fig. 6. From the figure one sees that the ratio for the G-parity odd part is very close to unity for $r>2.5$ fm, with the pion mass 140 MeV for the OBE. On the other hand, the G-parity even part is roughly fitted with the ρ meson mass 430 MeV in the region $r>2.5$ fm. Hence, the asymptotic form of the SS potential has the character of the one-π and -ρ exchange potential. Using these results, we obtain the coupling constants of the OBE potential predicted by the Skyrme model:

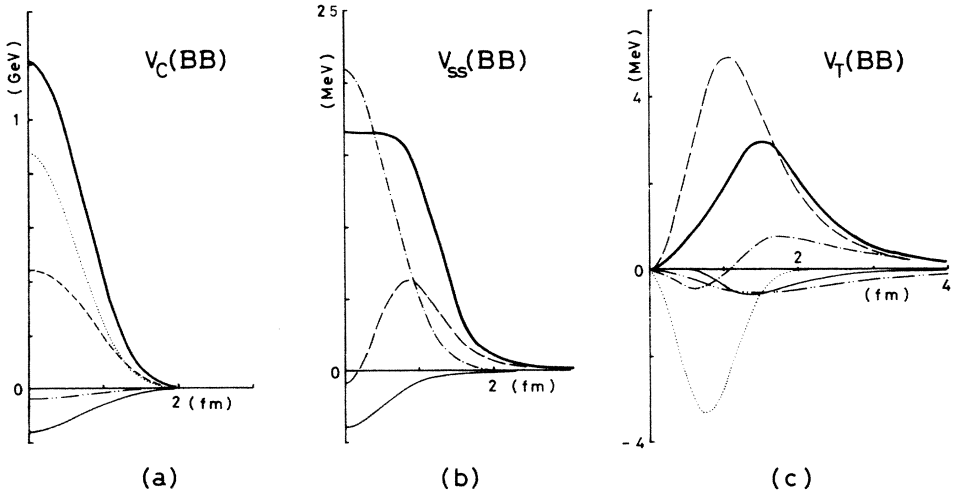

FIG. 5. The skyrmion-skyrmion potentials calculated for case II. (a), (b), and (c) are the central, V_c, the spin-spin, V_{ss}, and the tensor, V_T, parts, respectively. See the caption of Fig. 4 for details. The thin solid curves are the contributions from the term V_{4S}.

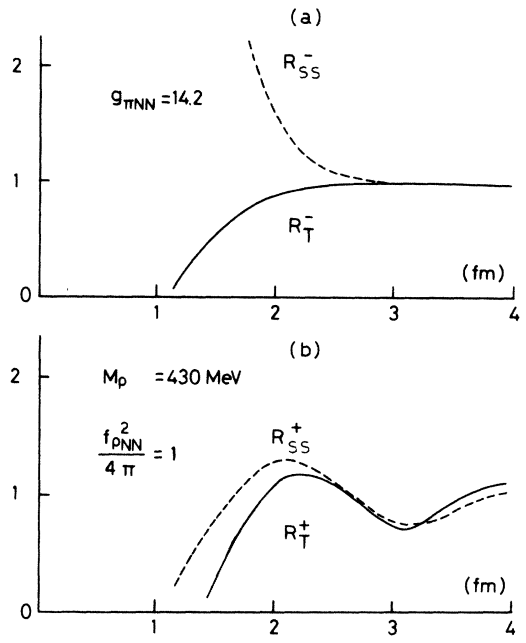

FIG. 6. The comparison of the present skyrmion-skyrmion potential for case I with the one-boson-exchange potential: (a) is the ratio of the G-parity odd part to the one-π exchange potential; (b) shows the ratio of the G-parity even part to the one-ρ-meson exchange potential. The dashed and solid curves show the results for the spin-spin and tensor components, respectively.

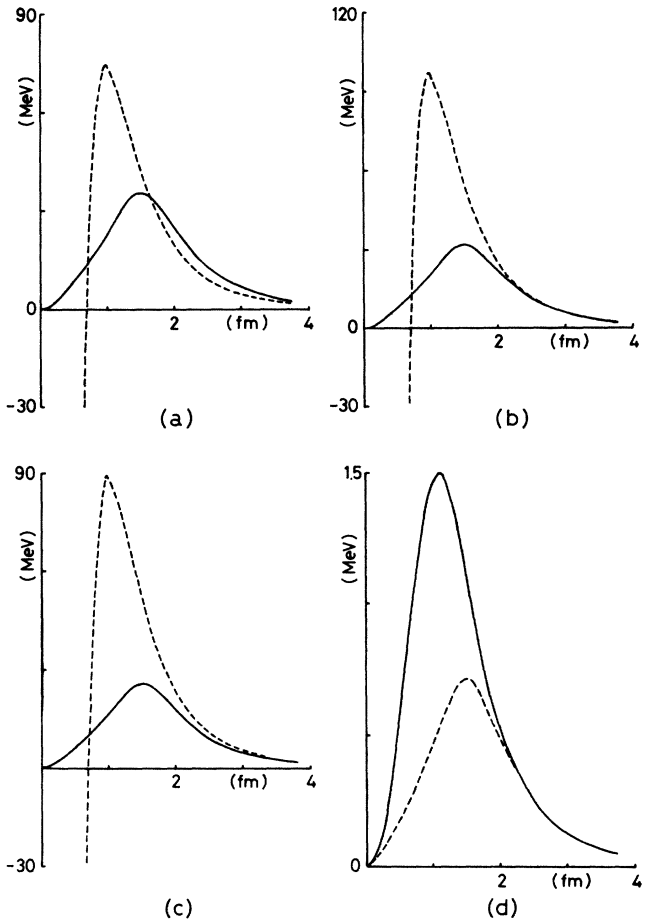

FIG. 7. The calculated transition potentials: (a), (b), and (c) are those between the $^1D_2$(NN) and $^5S_2$(NΔ), $^3F_3$(NN) and $^5P_3$(NΔ), and $^1G_4$(NN) and $^5D_4$(NΔ) states, respectively. The solid curves show the calculated results, and are compared with the phenomenological one-π and one-ρ exchange potentials (Ref. 24) shown by the dotted curves. (d) is the transition potential between the $^3P_2$(NΔ) and $^3F_2$(NΔ) states, where the solid curve shows the calculated transition potential with all the components but the dashed curve the potential calculated without the higher-rank tensor component V_T'.

$$\frac{g^2_{\pi NN}}{4\pi}=14.2,\quad m_\pi=140\ \text{MeV}\ ,$$
$$\frac{f^2_{\rho NN}}{4\pi}=1.0,\quad m_\rho=430\ \text{MeV}\ . \tag{4.4}$$

E. Transition potentials between NN and NΔ states

The SS potential can be projected onto the NN, NΔ, and ΔΔ potentials and also onto the transition potentials between them. These are calculated from the generalized potential in Eq. (3.17a) using the matrix elements of the operators Θ's. The explicit expressions for the matrix elements of these operators are summarized in Appendix B. Figure 7 shows the transition potential $V_{\text{NN,N}\Delta}(r)$ calculated for case I: The solid curves in Figs. 7(a), 7(b), and 7(c) display those between the $^1D_2$(NN) and $^5S_2$(NΔ), $^3F_3$(NN) and $^5P_3$(NΔ), and $^1G_4$(NN) and $^5D_4$(NΔ) states, respectively. For the sake of comparison, we also show the transition potentials calculated for the one-π and -ρ exchange potential[24] by the dashed curves. Here, the dipole-type cutoff was used to calculate them. One can see from the figures that the prediction of the Skyrme model is very similar to that of the one-boson-exchange potential. It can be said that the Skyrme model automatically includes a kind of cutoff function and also the contribution from the π and ρ exchanges in the asymptotic region.

Here, we mention the contribution from the higher rank tensor terms in the potential. These terms contribute for the states involving the Δ isobar, since the operators are the second-rank tensors of the spin and isospin operators. The terms are usually small, but may contribute a large effect for some states. For example, the value of the matrix element of Θ_T' between the $^3P_2$(NΔ) and $^3F_2$(NΔ) states is much larger than that of Θ_T. As a consequence, the V_T' part becomes comparative to the V_T part. In Fig. 7(d) the solid curve shows the potential between the $^3P_2$(NΔ) and $^3F_2$(NΔ) states calculated by including all the contributions, and the dashed curve shows that without the V_T' part.

Finally, we show an effect of the channel coupling including the NN, NΔ, and ΔΔ states for the scattering phase shifts. For the $^1D_2$(NN) state, for example, the calculated phase shift is increased by 3 deg at 50 MeV and by 13 deg at 250 MeV by the channel-coupling effect. Hence, the channel coupling contributes an attractive but not so large effect to the interaction.

V. DISCUSSIONS AND SUMMARY

In this paper we examined a modified Skyrme model in which the symmetric quartic term $\mathcal{L}_{4S}$ and the ω-coupling term $\mathcal{L}_6$ are both included in addition to the terms of the pure Skyrme model. The term $\mathcal{L}_6$ is the infinitely large limit of the ω-meson mass in an ω-coupling term, which was introduced by Jackson *et al.*[8] We studied the static properties of the nucleon in this modified Skyrme model. The coupling constants of the model were chosen so as to reproduce the $\pi\pi$ scattering data and the static properties of the nucleon as well as possible. Two kinds of parameter sets were chosen; one of the sets (case I) is obtained without the $\mathcal{L}_{4S}$, and the other with it. It was shown that the static properties of the nucleon are well reproduced for both cases; the model nicely reproduces the magnetic moment, the charge form factor, and also the axial coupling constant g_A compared with those of the pure Skyrme model.[2]

We next investigated the skyrmion- (anti-) skyrmion (SS or $S\bar{S}$) potential within the above model. It was shown that the potential can be written by means of the generalized spin and isospin operators. The resulting potential is easily projected onto those for the physical states with a definite spin and isospin configuration. Hence, we obtain the NN, NΔ, and $\Delta\Delta$ potentials and the transition potentials between these states from the SS potential.

We found that the SS potential has a good correspondence with the one-boson-exchange (OBE) potential of the π and ρ mesons in the long distance region ($r > 2.5$ fm). We extracted the effective coupling constants and the masses of the π and ρ mesons. They are consistent with the phenomenological ones and also with the previous results of the pure Skyrme model without the term $\mathcal{L}_6$. This means that the asymptotic form of the SS potential is almost independent with what an effective Lagrangian has been employed. As for the central potential, one has a repulsive core about the nucleon mass. The contribution from the $\mathcal{L}_6$ term is the main part of the central potential in the short-range part and is given by the folding of the baryon densities. Its G-parity structure is odd and is like an ω-meson-exchange potential. However, the central potential shows no attraction at the intermediate region, where the phenomenological potential possesses an attractive contribution due to the "σ-meson" exchange. The $\mathcal{L}_{4S}$ term was expected to give rise to such a contribution, but the absence of the "σ-meson" exchange seems to be independent of including the term or not; actually, the contribution from the $\mathcal{L}_{4S}$ term is attractive, but not enough to compensate for the repulsive contribution from the $\mathcal{L}_6$.

As shown in Ref. 13, one could increase the value of the coupling constant γ of the $\mathcal{L}_{4S}$ term by also increasing the ω-coupling constant; the $\mathcal{L}_{4S}$ term is a destabilizer while the $\mathcal{L}_6$ is a stabilizer. In such a case we may have a sufficient attraction for the central potential. We tried a calculation with the parameter set $e=10$, $F_\pi=130$ MeV, $\gamma=0.35$, and $g_\omega^2/4\pi=30.0$. The result shows, however, no attractive part. This may be considered to be in contradiction with the calculation in Ref. 13, in which a strongly attractive contribution to the potential was found. However, an additive ansatz was used for the ω-meson field. We see that the component $V_6^{\rm II}$ from the $\mathcal{L}_6$ term has been completely neglected by this ansatz. $V_6^{\rm II}$ is very large in the intermediate region of the central potential and masks the attractive contribution from the $\mathcal{L}_{4S}$ term. Therefore, the "σ-meson" contribution cannot be explained by including the $\mathcal{L}_{4S}$.

Here, we comment on the role of the $\mathcal{L}_{4S}$ term. We have the inequality [given by Eq. (2.8)] of the coupling constants to obtain a stable solution of the unit baryon number. Increasing the baryon number, however, the allowed value of γ becomes smaller and smaller: For example, for the case $F_\pi=130$ MeV, $e=10.0$, and $g_\omega^2/4\pi=10.0$, the critical γ_c is 0.43, 0.15, and 0.06 for the baryon numbers $n=1$, 2, and 3, respectively. Therefore, the inclusion of the $\mathcal{L}_{4S}$ term creates a serious problem. The term may be considered a large mass limit of a scalar meson coupling term,[13] but such an instability problem for a multiskyrmion system cannot be avoided by introducing a finite mass effect of the scalar meson. When we consider, in the skyrmion physics, that an effective Lagrangian of mesons should support stable soliton solutions, we face the problem of how the S-wave $\pi\pi$ scattering is consistently described in the meson Lagrangian without throwing out stable soliton solutions. We may need to abandon the product ansatz for the two-skyrmion field. When we include the ω-coupling term, the effect of the deformation from the spherically symmetric hedgehog solution may become large. Here, it should be noted that a finite mass effect of the ω-meson mass will instead smooth out the potential obtained from the contribution. Thus, the range of the repulsive core becomes large, the situation being worse. It is, on the other hand, interesting to study the role of vector mesons such as the ρ and A_1 mesons in the SS interaction.

APPENDIX A: THE STRONG COUPLING RELATION

In the strong coupling theory of a meson-baryon system, the Lie-group G is the semidirect product of the nine-parameter Abelian group T_9 and the spin-flavor $SU(2)_J \times SU(2)_I$ group.[18,19] $D_{\mu\tau}$ in Eq. (2.10) can be interpreted as the meson currents in the theory because they transform like the regular representation under the $SU(2)_J \times SU(2)_I$ as follows:

$$\begin{aligned}
&[J_\pm, D_{\mu\tau}] = \sqrt{(1\mp\mu)(2\mp\mu)}\, D_{\mu\mp1,\tau}\ , \\
&[J_z, D_{\mu\tau}] = \mu D_{\mu\tau}\ , \\
&[J_\pm, D_{\mu\tau}] = \sqrt{(1\mp\tau)(2\pm\tau)}\, D_{\mu,\tau\pm1}\ , \\
&[I_z, D_{\mu\tau}] = \tau D_{\mu\tau}\ .
\end{aligned} \tag{A1}$$

The strong coupling relation is given by the commutation relation

$$[D_{\mu\tau}, D_{\mu'\tau'}] = 0\ . \tag{A2}$$

Following Singh,[19] let us denote the isobar states by ϕ^j_{mt}, where j is the spin and m and t are the third components of the spin and isospin, respectively. Then, using Eq. (A1) and the Wigner-Eckart theorem, we obtain

$$(\phi^{j'}_{m't'}, D_{\mu\nu}\phi^{j}_{mt}) = \frac{1}{2j'+1}(jm\,|\,\mu\,|\,j'm')(j\pm 1\,\mu\nu\,|\,j't')(j'||D||j)\ . \tag{A3}$$

By using Eq. (A2), the reduced matrix element is given by

$$(j'||D||j)=\hat{j}'\hat{j}\ , \tag{A4}$$

where we normalized the element by noting that $D_{\mu\tau}$ is an orthogonal matrix in the Cartesian representation. Using (A3) and (A4), we finally obtain Eq. (3.16b).

APPENDIX B: MATRIX ELEMENTS OF Θ_{ss}, Θ_T, Θ'_{ss}, AND Θ'_T

In this appendix we give the matrix elements of the spin-isospin operators Θ_{ss}, Θ_T, Θ'_{ss}, and Θ'_T between the NN, NΔ, and ΔΔ states, which appeared in the skyrmion-skyrmion interaction potential in Eq. (3.17a). The operators Θ_{ss} and Θ_T are the same as the usual $\mathbf{S}\cdot\mathbf{S}\,\mathbf{T}\cdot\mathbf{T}$ and tensor operators, where $\mathbf{S}$ and $\mathbf{T}$ are the generalized spin and isospin operators. The matrix element of Θ_{ss} is written as

$$\langle\{B_1(s_1t_1)B_2(s_2t_2)\}(s_3t_3)\,|\,\Theta_{ss}\,|\,\{B'_1(s'_1t'_1)B'_2(s'_2t'_2)\}(s'_2t'_2)\rangle = 9\Lambda(B_1,B'_1)\Lambda(B_2,B'_2) \times\langle(s_1s_2)s_3\,|\,\mathbf{S}\cdot\mathbf{S}\,|\,(s'_1s'_2)s'_3\rangle\langle(t_1t_2)j_3\,|\,\mathbf{T}\cdot\mathbf{T}\,|\,(t'_1t'_2)j'_3\rangle\ , \tag{B1}$$

where $B_1(s_1t_1)$ denotes an isobar with the spin s_1 and isospin t_1 (note $s_1=t_1$); s_3 and t_3 are the total spin and isospin in the state. The $\Lambda(B_1,B'_1)$'s are the reduced matrix elements given by Eq. (3.16b). The matrix element of Θ'_{ss} is given by

$$\begin{aligned}&\langle\{B_1(s_1t_1)B_2(s_2t_2)\}(s_3t_3)\,|\,\Theta'_{ss}\,|\,\{B'_1(s'_1t'_1)B'_2(s'_2t'_2)\}(s'_3t'_3)\rangle\\ &=225\sum_{B''_1,B''_2}\Lambda(B_1,B''_1)\Lambda(B''_1,B'_1)\Lambda(B_2,B''_2)\Lambda(B''_2,B'_2)\langle t_1||\mathbf{S}||t''_1\rangle^2\langle t''_1||\mathbf{S}||t'_1\rangle^2\langle t_2||\mathbf{S}||t''_2\rangle^2\langle t''_2||\mathbf{S}||t'_2\rangle^2\\ &\quad\times\begin{Bmatrix}t'_1 & t_1 & 2\\ 1 & 1 & t''_2\end{Bmatrix}^2\begin{Bmatrix}t'_2 & t_2 & 2\\ 1 & 1 & t''_2\end{Bmatrix}^2\langle(s_1s_2)s_3\,|\,\mathbf{S}^{(2)}\cdot\mathbf{S}^{(2)}\,|\,(s'_1s'_2)s'_3\rangle\langle(t_1t_2)t_3\,|\,\mathbf{T}^{(2)}\cdot\mathbf{T}^{(2)}\,|\,(t'_1t'_2)t'_3\rangle\ .\end{aligned} \tag{B2}$$

For Θ_T we find

$$\begin{aligned}&\langle\{B_1(s_1t_1)B_2(s_2t_2)\}(s_3t_3)\lambda J\,|\,\Theta_T\,|\,\{B'_1(s'_1t'_1)B'_2(s'_2t'_2)\}(s'_3t'_3)\lambda' J\rangle\\ &\quad=9\Lambda(B_1,B'_1)\Lambda(B_2,B'_2)\langle\{(s_1s_2)s_3\lambda\}J\,|\,S_{12}\,|\,\{(s'_1s'_2)s'_3\lambda'\}J\rangle\langle(t_1t_2)t_3\,|\,\mathbf{T}\cdot\mathbf{T}\,|\,(t'_1t'_2)t'_3\rangle\ ,\end{aligned} \tag{B3}$$

where λ denotes the relative orbital angular momentum and $\mathbf{J}=\boldsymbol{\lambda}+\mathbf{s}_3$ the total. For Θ'_T we find

$$\begin{aligned}&\langle\{B_1(s_1t_1)B_2(s_2t_2)\}(s_3t_3)\lambda J\,|\,\Theta'_T\,|\,\{B'_1(s'_1t'_1)B'_2(s'_2t'_2)\}(s'_3t'_3)\lambda' J\rangle\\ &=-9\times5^3\begin{Bmatrix}2 & 2 & 2\\ 1 & 1 & 1\end{Bmatrix}\sum_{B''_1,B''_2}\Lambda(B_1,B''_1)\Lambda(B''_1,B'_1)\Lambda(B_2,B''_2)\Lambda(B''_2,B'_2)\\ &\quad\times\langle t_1||\mathbf{S}||t''_1\rangle^2\langle t''_1||\mathbf{S}||t'_1\rangle^2\langle t_2||\mathbf{S}||t''_2\rangle^2\langle t''_2||\mathbf{S}||t'_2\rangle^2\begin{Bmatrix}t'_1 & t_1 & 2\\ 1 & 1 & t''_2\end{Bmatrix}^2\begin{Bmatrix}t'_2 & t_2 & 2\\ 1 & 1 & t''_2\end{Bmatrix}^2\\ &\quad\times\langle\{(s_1s_2)s_3\lambda\}J\,|\,S^{(2)}_{12}\,|\,\{(s'_1s'_2)s'_3\lambda'\}J\rangle\langle(t_1t_2)t_3\,|\,\mathbf{T}^{(2)}\cdot\mathbf{T}^{(2)}\,|\,(t'_1t'_2)t'_3\rangle\ .\end{aligned} \tag{B4}$$

In the above, we have

$$\langle(s_1s_2)s_3\,|\,\mathbf{S}^{(i)}\cdot\mathbf{S}^{(i)}\,|\,(s'_1s'_2)s'_3\rangle=\delta_{s_3s'_3}(-)^{s_3+s_2+s'_1}\begin{Bmatrix}s_1 & s_2 & s_3\\ s'_2 & s'_1 & 1\end{Bmatrix}\langle s_1||\mathbf{S}^{(i)}||s'_1\rangle\langle s_2||\mathbf{S}^{(i)}||s'_2\rangle \tag{B5}$$

and

$$\langle\{(s_1s_2)s_3\lambda\}J\,|\,S^{(i)}_{12}\,|\,\{(s'_1s'_2)s'_3\lambda'\}J\rangle = (-)^{J+s'_3}3\sqrt{30}s\hat{s}_3\hat{s}'_3\hat{\lambda}\hat{\lambda}'\begin{bmatrix}\lambda' & 2 & \lambda\\ 0 & 0 & 0\end{bmatrix}\begin{Bmatrix}\lambda & 2 & \lambda'\\ s'_3 & J & s_3\end{Bmatrix}\begin{Bmatrix}s_1 & s_2 & s_3\\ s'_1 & s'_2 & s'_3\\ i & i & 2\end{Bmatrix}\langle s_1||\mathbf{S}^{(i)}||s'_1\rangle\langle s_2||\mathbf{S}^{(i)}||s'_2\rangle\ , \tag{B6}$$

where

$$\langle s_1||\mathbf{S}^{(1)}||s_1'\rangle=\langle s_1||\mathbf{S}||s_1'\rangle,\quad \langle s_1||\mathbf{S}^{(2)}||s_1'\rangle=1\ ,$$

and (B7)

$$\langle s_1||\mathbf{S}||s_2\rangle=\begin{cases}\sqrt{6}, & s_1=s_2=\frac{1}{2}\\ 2\sqrt{15}, & s_1=s_2=\frac{3}{2}\\ 2, & \text{otherwise}\ .\end{cases}$$

The same formulas apply to the $\mathbf{T}^{(i)}\cdot\mathbf{T}^{(i)}$ term.

[1]T. H. R. Skyrme, Nucl. Phys. **31**, 556 (1962); E. Witten, *ibid.* **B223**, 422, 433 (1983).

[2]G. S. Adkins, C. R. Nappi, and E. Witten, Nucl. Phys. **B228**, 552 (1983); G. S. Adkins and C. R. Nappi, *ibid.* **B233**, 109 (1984).

[3]A. Jackson, A. D. Jackson, and V. Pasquir, Nucl. Phys. **A432**, 567 (1985).

[4]R. Vinh Mau, N. Lacombe, B. Loiseau, W. N. Cottingham, and P. Lisboa, Phys. Lett. **150B**, 259 (1985).

[5]V. Vento, Phys. Lett. **153B**, 198 (1985).

[6]H. Yabu and K. Ando, Prog. Theor. Phys. **74**, 750 (1985).

[7]T. Otofuji, T. Kurihara, H. Kanada, S. Saito, and M. Yasuno, Nagoya University Report No. DPNU-85-26, July, 1985 (unpublished).

[8]A. Jackson, A. D. Jackson, A. S. Goldhaber, G. E. Brown, and L. C. Castillejo, Phys. Lett. **154B**, 101 (1985).

[9]G. S. Adkins and C. R. Nappi, Phys. Lett. **137B**, 251 (1984).

[10]J. Gasser and H. Leutwyler, Phys. Lett. **125B**, 321 (1983).

[11]J. F. Donoghue, E. Golowich, and B. R. Holstein, Phys. Rev. Lett. **53**, 747 (1984).

[12]M. Lacombe, B. Loiseau, R. Vinh Mau, and W. N. Cottingham, Phys. Lett. **161B**, 31 (1985).

[13]M. Lacombe, B. Loiseau, R. Vinh Mau, and W. N. Cottingham, Phys. Lett. **169B**, 121 (1986).

[14]J. M. Eisenberg, A. Erell, and R. R. Silbar, Phys. Rev. C **33**, 1531 (1986).

[15]T. N. Pham and T. N. Truong, Phys. Rev. D **31**, 3025 (1985).

[16]M. Mashaal, T. N. Pham, and T. N. Truong, Phys. Rev. Lett. **56**, 436 (1986).

[17]T. Otofuji, S. Saito, M. Yasuno, H. Kanada, and T. Kurihara, Nagoya University Report No. DPNU-86-05, April, 1986 (unpublished).

[18]T. Cook, C. J. Goebel, and B. Sakita, Phys. Rev. Lett. **15**, 35 (1965).

[19]V. Singh, Phys. Rev. **144**, 1275 (1966).

[20]J.-L. Gerais and B. Sakita, Phys. Rev. Lett. **52**, 87 (1984); Phys. Rev. D **32**, 1795 (1984).

[21]K. Bardakci, Nucl. Phys. **B243**, 197 (1984).

[22]H. Sugawara and F. von Hippel, Phys. Rev. **172**, 1301 (1968).

[23]E. E. Chanbers and R. Hofstadter, Phys. Rev. **103**, 1454 (1956).

[24]T. Otofuji, K. Sakai, H. Kanada, S. Saito, and M. Yasuno, Prog. Theor. Phys. **73**, 703 (1985).